

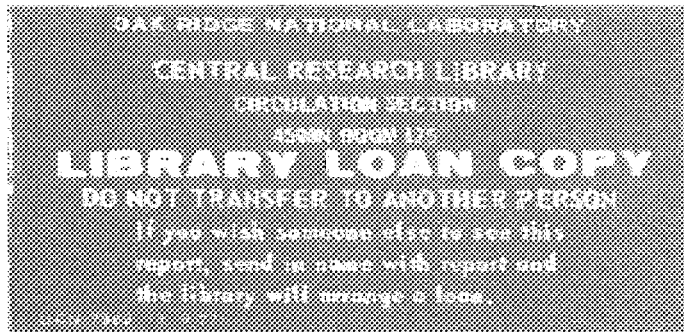
ORNL/TM-10872

**OAK RIDGE
NATIONAL
LABORATORY**

MARTIN MARIETTA

Interior Viewing of Complex Vacuum Vessels

R. N. Morris



OPERATED BY
MARTIN MARIETTA ENERGY SYSTEMS, INC.
FOR THE UNITED STATES
DEPARTMENT OF ENERGY

Printed in the United States of America. Available from
National Technical Information Service
U.S. Department of Commerce
5285 Port Royal Road, Springfield, Virginia 22161
NTIS price codes—Printed Copy: A02 Microfiche: A01

This report was prepared as an account of work sponsored by an agency of the United States Government. Neither the United States Government nor any agency thereof, nor any of their employees, makes any warranty, express or implied, or assumes any legal liability or responsibility for the accuracy, completeness, or usefulness of any information, apparatus, product, or process disclosed, or represents that its use would not infringe privately owned rights. Reference herein to any specific commercial product, process, or service by trade name, trademark, manufacturer, or otherwise, does not necessarily constitute or imply its endorsement, recommendation, or favoring by the United States Government or any agency thereof. The views and opinions of authors expressed herein do not necessarily state or reflect those of the United States Government or any agency thereof.

ORNL/TM-10872

Dist. Category UC-427

Computing and Telecommunications Division

**INTERIOR VIEWING OF
COMPLEX VACUUM VESSELS**

R. N. Morris

Date Published: September 1988

Prepared by the
OAK RIDGE NATIONAL LABORATORY
Oak Ridge, Tennessee 37831
operated by
MARTIN MARIETTA ENERGY SYSTEMS, INC.
for the
U.S. DEPARTMENT OF ENERGY
under contract DE-AC05-84OR21400



3 4456 0283139 0

CONTENTS

ABSTRACT	v
1. INTRODUCTION	1
2. VACUUM VESSEL MODEL	2
3. THE RAY-TRACING MODEL	3
4. CONCLUSIONS	6
REFERENCES	10

ABSTRACT

A ray-tracing and vacuum vessel modeling technique that allows one to generate a view looking into a complex vacuum vessel port is described. The technique is general enough so that details of the contained plasma can be seen as well as the vacuum vessel walls.

1. INTRODUCTION

Viewing the interior of vacuum vessels is important in the experimental alignment and data analysis of complex fusion energy experiments, such as the Advanced Toroidal Facility (ATF).¹ Vacuum vessels such as the one for ATF are complex in design and have few ports that offer an unobstructed view of the plasma under study at all angles of experimental interest. The ATF vacuum vessel is shown in Fig. 1. The goal of this computational viewing is to “look” through a vessel port and determine what a diagnostic sensor will “see” or what portion of the vacuum vessel a probe or beam will intersect. Ideally, one should include not only the vacuum vessel geometry but a plasma model as well so that the physics of the diagnostics can be addressed. Ray tracing has been chosen as the preferred technique because it has the ability to handle complex shapes and interfaces between one region (vacuum) and another (plasma). Ray tracing also simulates the physical operation of many devices of interest and can play a direct role in the analysis and modeling of an experimental diagnostic. Previously, diagnostics were aligned by an examination of the engineering drawings and simple geometric calculations. Though simple and

ORNL-DWG 85-3623 FED

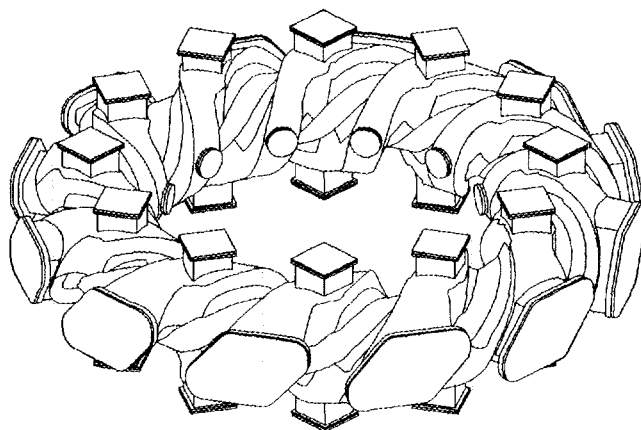


Fig. 1. ATF vacuum vessel.

straightforward, such methods are often not successful on complex vacuum vessels that do not contain a direction of symmetry, such as ATF. This report demonstrates how a more powerful technique, ray tracing, can solve the general alignment problem in complex situations.

2. VACUUM VESSEL MODEL

Inherent in the structure of the ray-tracing model are the details of the vacuum vessel. The method of representing the vacuum vessel under study is to use a "sliced" model. The vessel coordinates are transformed to cylindrical coordinates and the vacuum vessel is "sliced" at constant ϕ values to form a set of two-dimensional cross sections (ϕ is the toroidal angle). The number of cross sections is chosen so that the change from one cross section to another is small, and the number of points in each given cross section is selected so that all the necessary details of the vacuum vessel can be represented. This is illustrated in Fig. 2. The

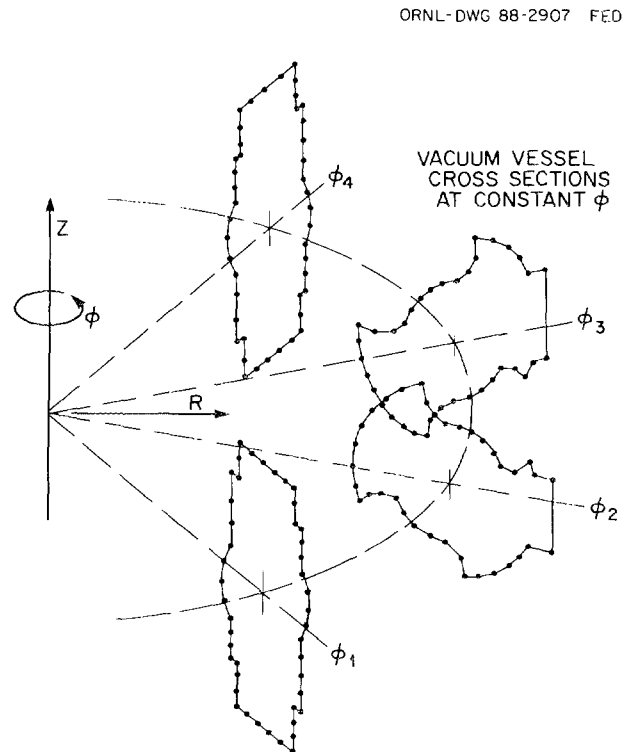


Fig. 2. Sliced model of the ATF vacuum vessel.

ATF vacuum vessel studied in this report had a periodic structure so that only one period needed to be modeled; typically, about 120 cross sections per period with 60 points each were required for good accuracy.

This model has the advantage that it is easy to modify a given cross section to include such things as ports and divertors; it has the disadvantage that the connectivity between cross sections is not preserved unless special care is taken. Fortunately for the purposes of this report, the connections between different cross sections can be approximated with good accuracy by choosing the nearest data point on a neighboring cross section.

3. THE RAY-TRACING MODEL

The principle of the ray-tracing model is quite simple and general (see Fig. 3). A view plane is established at the diagnostic location, and a grid is superimposed over its viewing aperture. Behind the view plane is an origin point for the rays

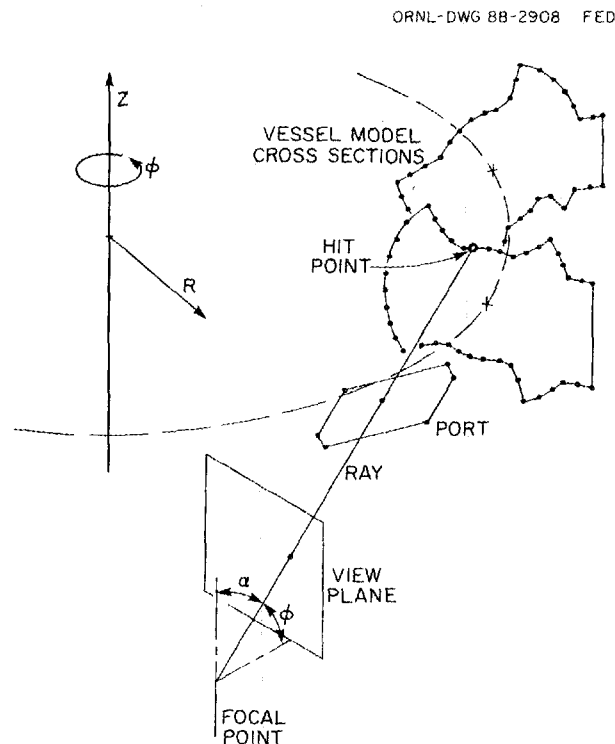


Fig. 3. Fundamental outline of the ray-tracing model.

which corresponds to the focal point or a pseudo focal point for the diagnostic. A ray is started at the view plane at two predetermined angles, θ and α . The two angles are determined from the characteristics of the device under study and the number of pixels desired in the view plane. The intersection point of the ray and the vessel port plane is then determined. If the ray is not within the port opening, that fact is recorded and a new ray started. Should the ray fall within the port opening, a stepping process is begun. The ray is advanced a small step, and this new position is examined to see if it is still within the vacuum vessel. This is done by examining the path coordinates of the ray.

The R , Z , and ϕ coordinates of the ray are calculated, and the ϕ value is rounded off to the nearest discrete value of the vacuum vessel cross-section set. Next, it is determined if the ray location is within the cross section. If so, the stepping process is continued. Should the point lie outside the cross section, a “hit” is recorded. The hit point is approximated as the point halfway between the last point known to be inside the vacuum vessel and the current “outside” point. The stepping increment is adjusted to be of the same order as the distance between the vessel cross sections. In general, a variable increment could be used to save time, but, because of the complex testing required, a fixed increment was used in this work.

The angles θ and α are varied in small steps over a range characteristic of the view angles of the diagnostic under study so that the view plane is completely scanned. Typically, a grid of 128 by 128 pixels is formed on the view plane, each with its own intensity value as determined by tracing the appropriate ray. The intensity variation of the pixels over the view plane is what forms the picture of the view.

The intensity of the reflection from the hit point is

$$I = \frac{(\hat{r} \cdot \hat{n})^m}{R^n}, \quad (1)$$

where \hat{r} is the unit vector in the ray direction, \hat{n} is the unit vector perpendicular to the vessel surface, R is the distance from the view plane to the hit point, and m and n are exponents used to enhance the details of the wall.^{2,3} The unit vector perpendicular to the wall is determined by forming the cross product between a vector that lies on a cross section and a vector that connects two cross sections. The first vector is formed by finding the two-cross section points (on the nearest discrete cross section) that straddle the hit point. The second vector is formed by

finding the nearest points to the hit point on both the nearest cross section and a nearby cross section (see Fig. 4). In general, the best method would be to preserve the connectivity between cross sections and use it to form the second vector, but the method used in this work gives good results with simpler data sets.

The view picture is formed by plotting the logarithm of the intensity because this models the intensity profiles as processed by the eye. Each intensity point on the view plane is treated as a pixel, with a gray scale from 0 to 13, 13 being black. An expanded gray scale would be useful, but currently this work is limited to a gray scale of approximately 13 by the available output devices. The m and n values are chosen to enhance the desired characteristics of the picture. The theory of homomorphic signal processing allows us to identify the numerator of Eq. (1) as a function that changes rapidly and can be associated with edges. The denominator can be observed to change more slowly and can be identified as an illumination function. Changing the n and m values allows us to accent or reduce the qualities of the picture.³ A small n value provides dynamic range compression, and a large m number provides edge definition. In practice, $m = 6$ and $n = 1$ are useful. See Fig. 5 for the layout of the optics and Fig. 6 for a composite picture.

ORNL-DWG 88-2909 FED

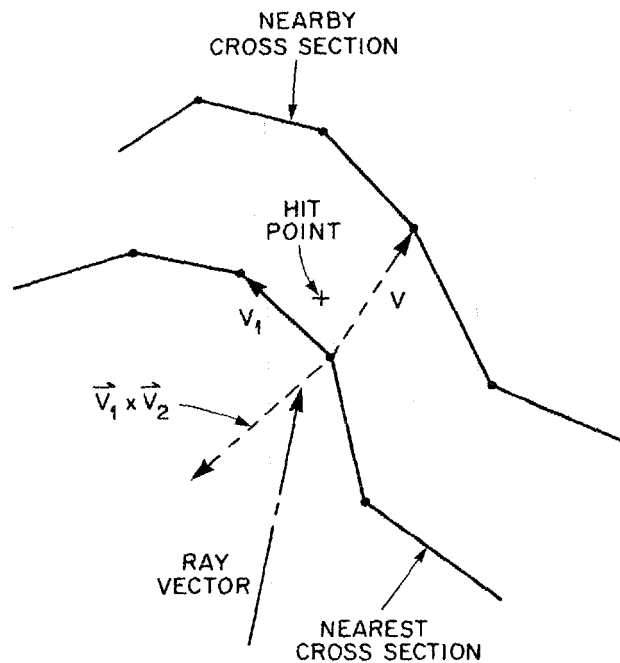


Fig. 4. Determination of the vector perpendicular to the vacuum vessel wall.

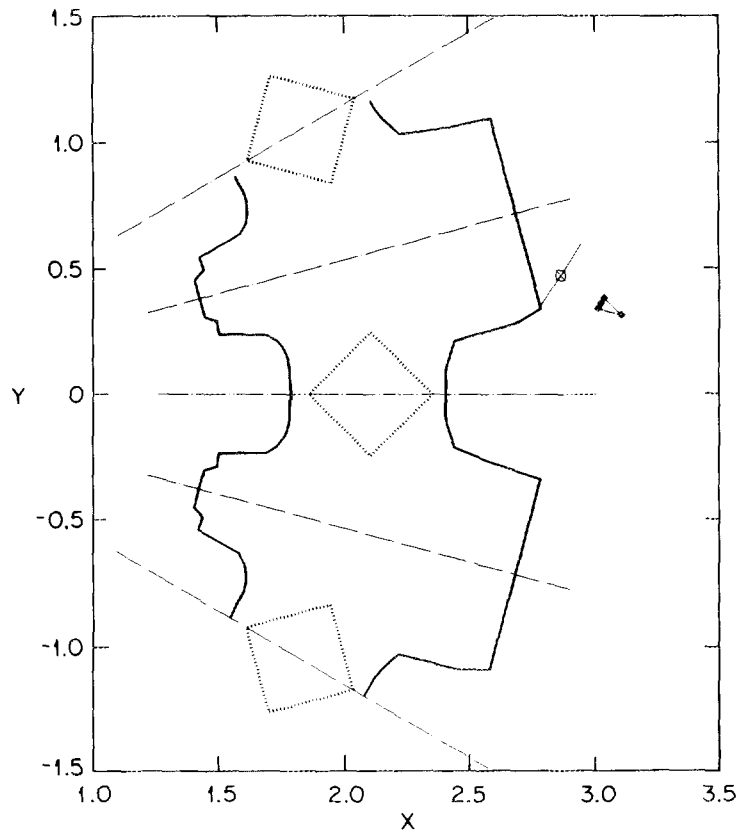


Fig. 5. Midplane view of the diagnostic geometry.

Figure 5 is the layout of the diagnostic geometry. The dark, solid lines show the vacuum vessel at its midplane. The cone-shaped object is the view plane and its focal point; the view angle is looking into the vacuum vessel through a large side port. Figure 6 is the view as seen by the diagnostic as located in Fig. 5. Notice the corkscrew appearance of the picture, along with the fact that the coil troughs (“corkscrews”) hinder complete access to the plasma. The quality of the picture may be improved by using more grid points and a greater number of intensity levels at the expense of greater computational effort.

4. CONCLUSIONS

Ray tracing, along with the sliced vacuum vessel model, provides useful tools for the interior viewing of complex vacuum vessels. Variations on this theme are

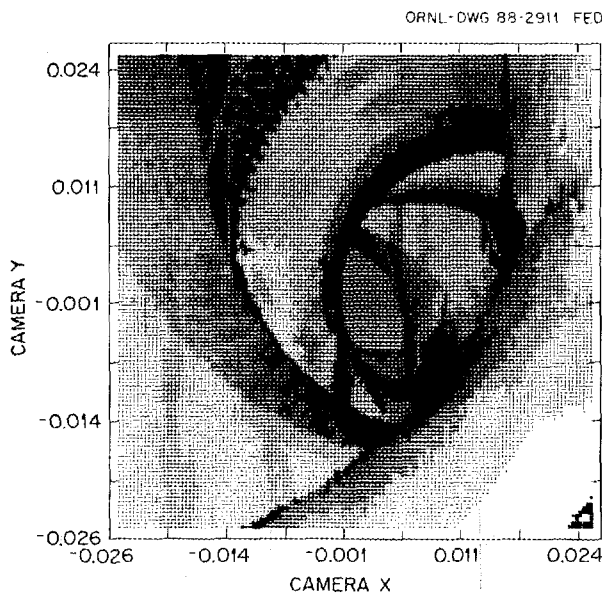


Fig. 6. Picture of the vacuum vessel interior as generated by the algorithm of the report.

possible. For example, one can place a view screen within the vacuum vessel and step the ray to the view screen, rather than to the far wall, to examine interior plasma details. This would allow one to examine the portion of a plasma profile that could be seen by a diagnostic looking in.⁴ Another possibility is to model the injection of a beam into the plasma with the wall hits serving to model beam-wall interactions.⁵ In all these cases, the ray tracing is able to deal with the complex geometry and is limited only by the details of the physics models.

This method is easily applied to the plasma as well as to the vacuum vessel interior. Figure 7 is a view of the plasma as seen from the position shown in Fig. 5. The method used is the same as for the vacuum vessel except that a hit is recorded when the ray is inside the plasma. Figure 8 shows how rf energy is deposited within the plasma. The rf energy is assumed to be evenly distributed throughout the plasma and to be absorbed by the plasma when it encounters a critical value of the magnetic field. In this case, the ray tracing proceeds by following the ray through the vacuum vessel and plasma until it encounters a region where the magnetic field has the critical value. A pixel intensity is generated by dividing the normalized plasma density at that point by the distance from the view plane. Of course, the usual wall interference is also included in the process.

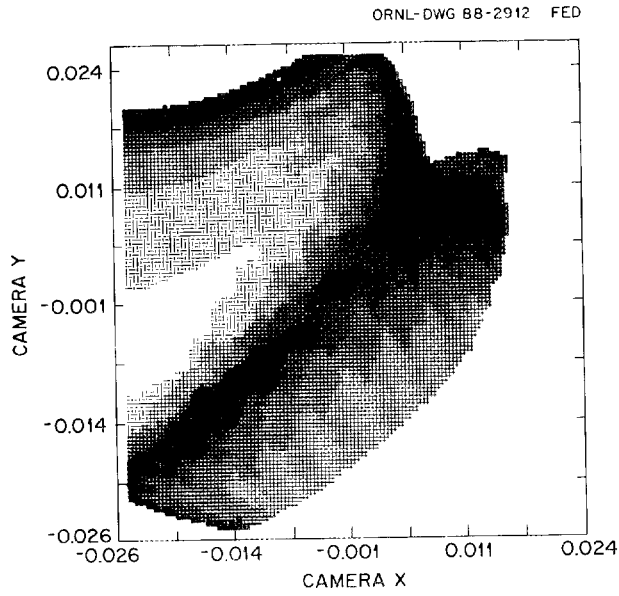


Fig. 7. Picture of the plasma exterior.

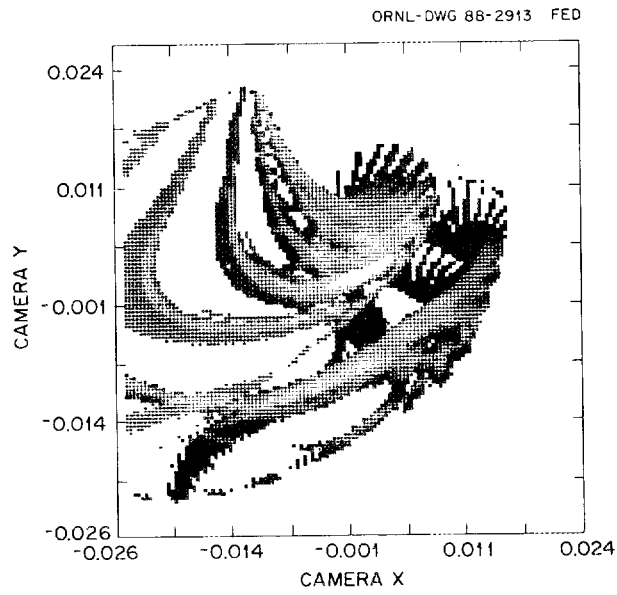


Fig. 8. Picture of the rf power deposition.

Finally, it is also possible to use this technique to examine the view of a cross section of the plasma. Figures 9 and 10 show how a cross section of the plasma appears to the Thomson scattering light collector on ATF.⁴ Figure 9 is the geometry of the detector layout (the same as Fig. 5), with the horizontal, dark, solid line in the vacuum vessel forming the view plane. The crosses in Fig. 10 are points that can be seen with no interference from the wall. The large outer ellipse is the boundary of the plasma, and the boxlike outline is the vacuum vessel cross section. In this case, one draws a ray from a point on the desired cross section to the view point and steps a ray along it as before.

As can be seen, this ray-tracing technique is quite general and can be applied to a large number of possible configurations.

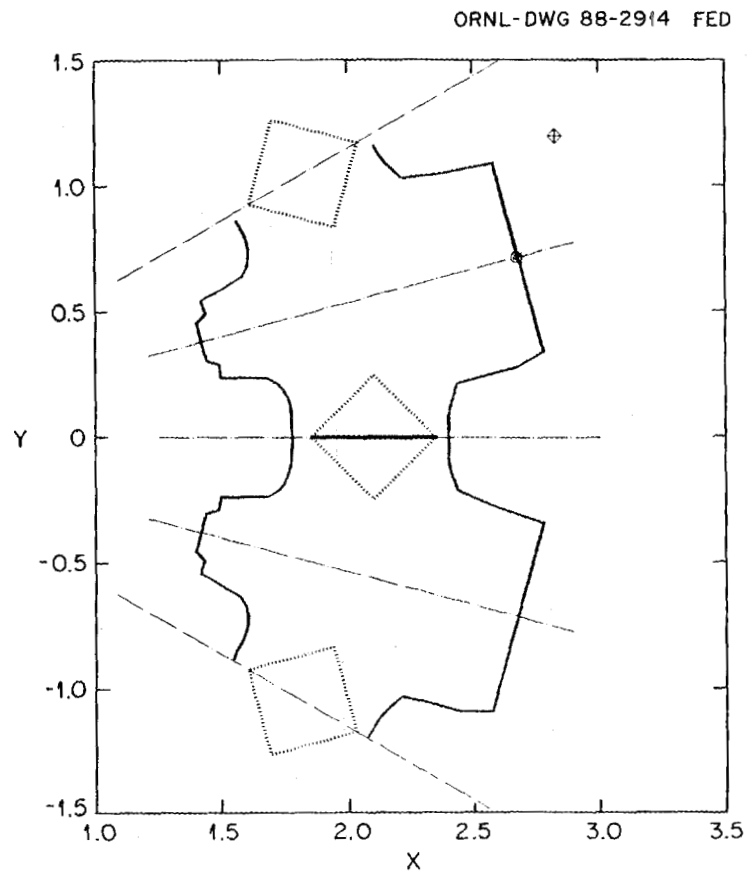


Fig. 9. Midplane view of the Thomson scattering light collector.

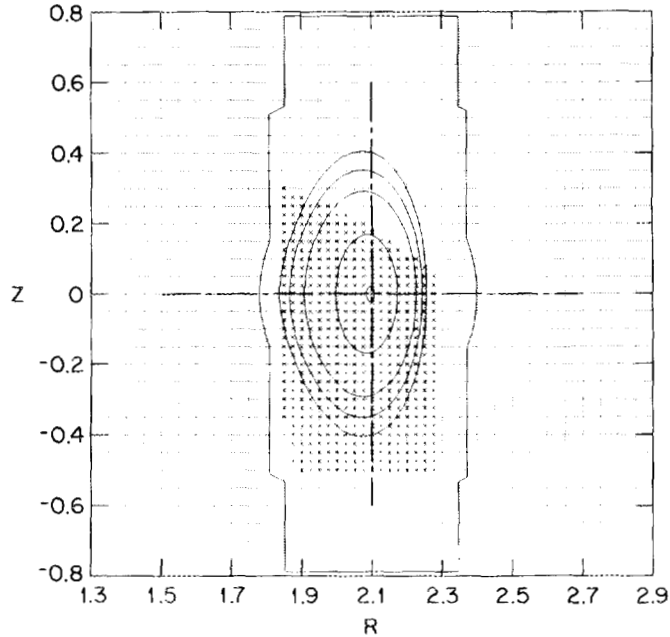


Fig. 10. Cross-sectional view of a plasma plane in ATF. The "x's" are points that can be seen with no wall interference.

REFERENCES

1. J. F. Lyon, B. A. Carreras, K. K. Chipley, M. J. Cole, J. H. Harris, T. C. Jernigan, R. L. Johnson, V. E. Lynch, B. E. Nelson, J. A. Rome, J. Sheffield, and P. B. Thompson, "The Advanced Toroidal Facility," *Fusion Technol.*, **10**, 179 (1986).
2. Donald Hearn and M. Pauline Baker, *Computer Graphics*, Prentice-Hall, Englewood Cliffs, New Jersey, 1986.
3. Alan V. Oppenheim and Ronald W. Schafer, *Digital Signal Processing*, Prentice-Hall, Englewood Cliffs, New Jersey, 1975.
4. R. R. Kindsfather, D. A. Rasmussen, M. Murakami, C. E. Thomas, S. L. Painter, P. S. Hays, and R. N. Morris, "Two-Dimensional Thomson Scattering System for ATF," *Rev. Sci. Instrum.* **57** (8), 1816 (1986).
5. R. N. Morris, R. H. Fowler, J. A. Rome, and T. J. Schlagel, "Advanced Toroidal Facility Neutral Beam Injection: Optimization of Beam Alignment and Aperturing," *Fusion Technol.* **12**, 281 (1986).

ORNL/TM-10872

Dist. Category UC-427

INTERNAL DISTRIBUTION

- | | |
|--------------------|--|
| 1. D. B. Batchelor | 19. M. J. Saltmarsh |
| 2. C. O. Beasley | 20. K. C. Shaing |
| 3. B. A. Carreras | 21. J. Sheffield |
| 4. M. D. Carter | 22. D. A. Spong |
| 5. E. C. Crume | 23. G. E. Whitesides |
| 6. R. A. Dory | 24-25. Laboratory Records
Department |
| 7. J. L. Dunlap | 26. Laboratory Records,
ORNL-RC |
| 8. R. H. Fowler | 27. Document Reference
Section |
| 9. C. L. Hedrick | 28. Central Research Library |
| 10. S. P. Hirshman | 29. Fusion Energy Division
Library |
| 11. J. T. Hogan | 30-31. Fusion Energy Division
Publications Office |
| 12. W. A. Houlberg | 32. ORNL Patent Office |
| 13. H. C. Howe | |
| 14. E. F. Jaeger | |
| 15. G. S. Lee | |
| 16. J. F. Lyon | |
| 17. R. N. Morris | |
| 18. J. A. Rome | |

EXTERNAL DISTRIBUTION

33. Office of the Assistant Manager for Energy Research and Development, U.S. Department of Energy, Oak Ridge Operations Office, P.O. Box E, Oak Ridge, TN 37831
34. J. D. Callen, Department of Nuclear Engineering, University of Wisconsin, Madison, WI 53706-1687
35. J. F. Clarke, Director, Office of Fusion Energy, Office of Energy Research, ER-50 Germantown, U.S. Department of Energy, Washington, DC 20545
36. R. W. Conn, Department of Chemical, Nuclear, and Thermal Engineering, University of California, Los Angeles, CA 90024
37. S. O. Dean, Fusion Power Associates, Inc., 2 Professional Drive, Suite 248, Gaithersburg, MD 20879
38. H. K. Forsen, Bechtel Group, Inc., Research Engineering, P.O. Box 3965, San Francisco, CA 94119
39. J. R. Gilleland, L-644, Lawrence Livermore National Laboratory, P.O. Box 5511, Livermore, CA 94550
40. R. W. Gould, Department of Applied Physics, California Institute of Technology, Pasadena, CA 91125
41. R. A. Gross, Plasma Research Laboratory, Columbia University, New York, NY 10027
42. D. M. Meade, Princeton Plasma Physics Laboratory, P.O. Box 451, Princeton, NJ 08543
43. M. Roberts, International Programs, Office of Fusion Energy, Office of Energy Research, ER-52 Germantown, U.S. Department of Energy, Washington, DC 20545
44. W. M. Stacey, School of Nuclear Engineering and Health Physics, Georgia Institute of Technology, Atlanta, GA 30332

45. D. Steiner, Nuclear Engineering Department, NES Building, Tibbetts Avenue, Rensselaer Polytechnic Institute, Troy, NY 12181
46. R. Varma, Physical Research Laboratory, Navrangpura, Ahmedabad 380009, India
47. Bibliothek, Max-Planck Institut für Plasmaphysik, Boltzmannstrasse 2, D-8046 Garching, Federal Republic of Germany
48. Bibliothek, Institut für Plasmaphysik, KFA Jülich GmbH, Postfach 1913, D-5170 Jülich, Federal Republic of Germany
49. Bibliothek, KfK Karlsruhe GmbH, Postfach 3640, D-7500 Karlsruhe 1, Federal Republic of Germany
50. Bibliotheque, Centre de Recherches en Physique des Plasmas, Ecole Polytechnique Fédérale de Lausanne, 21 Avenue des Bains, CH-1007 Lausanne, Switzerland
51. R. Aymar, CEN/Cadarache, Departement de Recherches sur la Fusion Contrôlée, F-13108 Saint-Paul-lez-Durance Cedex, France
52. Bibliothèque, CEN/Cadarache, F-13108 Saint-Paul-lez-Durance Cedex, France
53. Library, Culham Laboratory, UKAEA, Abingdon, Oxfordshire, OX14 3DB, England
54. Library, JET Joint Undertaking, Abingdon, Oxfordshire OX14 3EA, England
55. Library, FOM-Instituut voor Plasmafysica, Rijnhuizen Edisonbaan 14, 3439 MN Nieuwegein, The Netherlands
56. Library, Institute of Plasma Physics, Nagoya University, Chikusa-ku, Nagoya 464, Japan
57. Library, International Centre for Theoretical Physics, P.O. Box 586, I-34100 Trieste, Italy
58. Library, Centro Recherche Energia Frascati, C.P. 65, I-00044 Frascati (Roma), Italy
59. Library, Plasma Physics Laboratory, Kyoto University, Gokasho, Uji, Kyoto 611, Japan
60. Plasma Research Laboratory, Australian National University, P.O. Box 4, Canberra, A.C.T. 2601, Australia
61. Library, Japan Atomic Energy Research Institute, Naka Fusion Research Establishment, 801-1 Mukoyama Naka-machi, Naka-gun, Ibaraki-ken, Japan
62. R. A. Blanken, Experimental Plasma Research Branch, Division of Applied Plasma Physics, Office of Fusion Energy, Office of Energy Research, ER-542, Germantown, U.S. Department of Energy, Washington, DC 20545
63. K. Bol, Princeton Plasma Physics Laboratory, P.O. Box 451, Princeton, NJ 08543
64. R. A. E. Bolton, IREQ Hydro-Quebec Research Institute, 1800 Monte Ste.-Julie, Varennes, P.Q. JOL 2P0, Canada
65. D. H. Crandall, Experimental Plasma Research Branch, Division of Applied Plasma Physics, Office of Fusion Energy, Office of Energy Research, ER-542, Germantown, U.S. Department of Energy, Washington, DC 20545
66. R. L. Freeman, GA Technologies, Inc., P.O. Box 85608, San Diego, CA 92138
67. K. W. Gentle, RLM 11.222, Institute for Fusion Studies, University of Texas, Austin, TX 78712

68. R. J. Goldston, Princeton Plasma Physics Laboratory, P.O. Box 451, Princeton, NJ 08543
69. J. C. Hosea, Princeton Plasma Physics Laboratory, P.O. Box 451, Princeton, NJ 08543
70. D. Markevich, Division of Confinement Systems, Office of Fusion Energy, Office of Energy Research, ER-55, Germantown, U.S. Department of Energy, Washington, DC 20545
71. R. H. McKnight, Experimental Plasma Research Branch, Division of Applied Plasma Physics, Office of Fusion Energy, Office of Energy Research, ER-542, Germantown, U.S. Department of Energy, Washington, DC 20545
72. E. Oktay, Division of Confinement Systems, Office of Fusion Energy, Office of Energy Research, ER-55, Germantown, U.S. Department of Energy, Washington, DC 20545
73. D. Overskei, GA Technologies, Inc., P.O. Box 85608, San Diego, CA 92138
74. R. R. Parker, Plasma Fusion Center, NW 16-288, Massachusetts Institute of Technology, Cambridge, MA 02139
75. W. L. Sadowski, Fusion Theory and Computer Services Branch, Division of Applied Plasma Physics, Office of Fusion Energy, Office of Energy Research, ER-541, Germantown, U.S. Department of Energy, Washington, DC 20545
76. J. W. Willis, Division of Confinement Systems, Office of Fusion Energy, Office of Energy Research, ER-55, Germantown, U.S. Department of Energy, Washington, DC 20545
77. A. P. Navarro, Division de Fusion, CIEMAT, Avenida Complutense 22, E-28040 Madrid, Spain
78. Laboratory for Plasma and Fusion Studies, Department of Nuclear Engineering, Seoul National University, Shinrim-dong, Gwanak-ku, Seoul 151, Korea
- 79-124. Given distribution as shown in OSTI-4500, Magnetic Fusion Energy (Category Distribution UC-427: Theoretical Plasma, Physics)

